6758–6769 *Nucleic Acids Research, 2003, Vol. 31, No. 23*
DOI: 10.1093/nar/gkg911

Cleavage of DNA without loss of genetic information by incorporation of a disaccharide nucleoside

Koen Nauwelaerts, Karen Vastmans, Matheus Froeyen, Veerle Kempeneers, Jef Rozenski, Helmut Rosemeyer[1], Arthur Van Aerschot, Roger Busson, Jeffrey C. Lacey, Ekaterina Efimtseva, Sergey Mikhailov, Eveline Lescrinier and Piet Herdewijn*

Rega Institute for Medical Research, Laboratory for Medicinal Chemistry, Minderbroedersstraat 10, B-3000 Leuven, Belgium and [1]Universität Osnabrück, Laboratory for Organic and Bioorganic Chemistry, Barbarastrasse 7, D-49069 Osnabrück, Germany

Received September 12, 2003; Revised and Accepted October 16, 2003

ABSTRACT

A ribose residue inserted between the 3′-OH of one nucleotide and the 5′-phosphate group of the next nucleotide, functions as a site-specific cleavage site within DNA. This extra ribose does not interrupt helix formation and it protects duplex DNA against cleavage by restriction enzymes. Cleavage can be obtained with periodate and all ribose fragments can be removed with sodium hydroxide. As a result of this, an intact natural oligodeoxynucleotide is obtained after ligation reaction, which means that site-specific cleavage and recovering of intact DNA occurs without loss of genetic information.

INTRODUCTION

Enzymes that cleave phosphodiester bonds of DNA play a crucial role in cell metabolism. Some of these enzymes cleave double-stranded DNA while others cleave single-stranded DNA. Double-stranded DNA can be cleaved at specific sites using restriction enzymes. These enzymes recognize specific sequences of four to eight bases producing dsDNA fragments with either blunt ends or sticky ends. Cohesive fragments produced by the same restriction enzyme can always be stuck together and joined permanently by the action of DNA ligase. This technique has played a major role in the development of recombinant DNA technology, i.e. the *in vitro*, site-specific genetic recombination. Type I topoisomerases are enzymes that catalyze the single-stranded cutting of dsDNA and produce changes in the supercoiling of DNA. Other topoisomerases (type II) cut both strands in a DNA double helix. As a chemical (non-enzymatic) alternative for this site-specific cleavage of DNA, we investigated the use of a disaccharide nucleotide.

DNA is built from nucleoside units connected via phosphodiester bonds between the 3′-position of one nucleoside and the 5′-position of the next nucleoside (Scheme 1). A possible way to introduce a cleavage site is to insert a chemical group (i.e. ribose) between the 3′-position of one nucleotide and the 5′-position of the other nucleotide. This chemical group should not interrupt helix formation and should be prone to chemical degradation. The cleavage reaction should result in the formation of two natural oligonucleotides (one with a free 3′-OH function and the other with a 5′-OPO_3H_2 group) so that both ends are available for a ligation reaction, when needed. This means that the complete ribose unit (or the entire alternative chemical groups) should be removed during the cleavage process. In this way, the cleavage reaction can be carried out without loss of a nucleotide fragment (no loss of genetic information). A molecule that might fulfil these criteria is 3′-O-β-D-ribofuranosyl-2′-deoxy nucleotides, incorporated in the 5′→5* direction (Scheme 1). Selective chemical degradation leading to DNA strand cleavage is used in the template-directed interference footprinting (1–4). In this case, however, several base-modified nucleotides are used to cover the whole spectrum of natural nucleotides involved.

MATERIALS AND METHODS

Preparation of the modified T*amidite

The modified building block (5) was phosphorylated with 2-cyanotethyl-*N,N*-diisopropylchlorophosporamidite analogous to previous procedures (6) following column chromatography with *n*-hexane/acetone/triethylamine (66:33:1) and precipitated in cold hexane, in 83% yield. R_f (*n*-hexane/acetone/triethylamine 49:49:2) 0.43. ^{31}P NMR ($CDCl_3$): 149.18; 149.86. ESI-MS (pos): 1055.4204 ($[C_{58}H_{63}N_4O_{13}P + H]^+$; calc. 1055.4207).

Oligonucleotide synthesis

Oligonucleotide synthesis was performed on an ABI 392A-DNA synthesizer (Applied Biosystems) by means of the phosphoramidite approach. The standard 1-μmol scale DNA assembly protocol was used, except for a 3 min coupling time with 0.12 M of the incoming amidite for the modified analogue. The standard 10 μmol scale protocol was used for the NMR oligo with 10 min coupling time for the modified amidite. The oligomers were deprotected and cleaved from the solid support by treatment with conc. aq. ammonia (50°C, 16 h). Following gel filtration on a NAP-10® column (Sephadex G25, DNA grade, Pharmacia), purification was

*To whom correspondence should be addressed. Tel: +32 16 337387; Fax: +32 16 337340; Email: Piet.Herdewijn@rega.kuleuven.ac.be

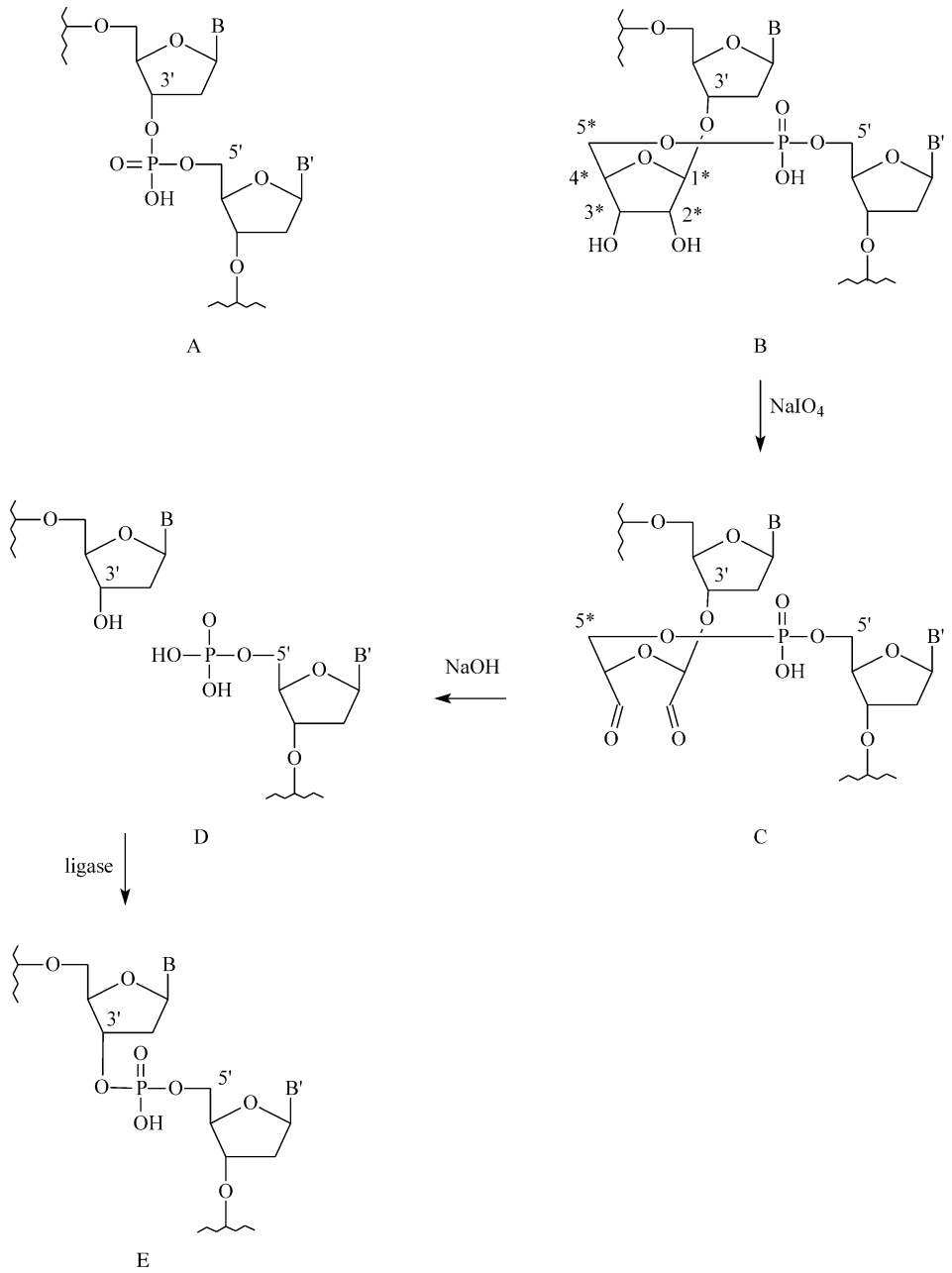

Scheme 1. Structure of a natural phosphodiester linkage (**A**) and of a 5′ → 5* phosphodiester linkage by inserting a ribose residue between two consecutive nucleotides (**B**). Also shown is the cleavage reaction using periodate (**C**) followed by degradation of the oxidized fragment with NaOH (**D**) and ligase of the resulting oligonucleotide fragment (**E**).

achieved on a Mono-Q®-HR-10/10 anion-exchange column (Pharmacia) with a $NaClO_4$ gradient in 0.2 M Tris–HCl buffer containing 10% of CH_3CN pH 7.0; the applied gradient depended on the oligomer; flow rate 2 ml min^{-1}. The product-containing fraction was desalted on a NAP-10® column and lyophilized.

Thermal stability studies

Oligomer concentrations were determined by measuring the absorbance in pure H_2O at 260 nm and 80°C and assuming the thymidine analogue to have the same extinction coefficient in the denatured state as thymidine. The extinction coefficients used were: dA, ε = 15 000; dT, ε = 8500; dG, ε = 12 500; dC, ε = 7500. T_m values were determined in a buffer containing 0.1 M NaCl, 0.02 M potassium phosphate (pH 7.5), 0.1 mM EDTA, with a 4 μM concentration for each strand. Melting curves were determined with a Cary-100-bio spectrophotometer. Cuvettes were maintained at constant temperature by means of water circulation through the cuvette holder. The temperature of the solution was measured with a thermistor directly immersed in one of the cuvettes. Temperature control and data acquisition were done automatically with an IBM-compatible computer. The samples were heated at a rate of 0.2°C min^{-1}, and no difference was observed between heating

1 5' GAGTCCATGG 3'

2 5' GAAACAGCTGAT*CCATGGACTC 3'

3 5' GAAACAGCTGATCCATGGACTC 3'

4 5' GAGTCCATGGATCAGCTGTTTC 3'

5 5' GAGTCCATGGAT*CAGCTGTTTC 3'

6 5' GAAACAGCTGAT 3'

7 5' CCATGGACTC 3'

8 5' GGCTTGATTCAAC 3'

9 5' GGCT*TGATT*CAAC 3'

10 5' GTTGAATCAAGCC 3'

Figure 1. Sequences of primers and templates used in the enzymatic reactions (1–7) as well as sequences used for T_m measurements which are not indicated in Table 1 (8–10). T* indicates the incorporated disaccharide nucleoside.

and cooling melting curves. Melting temperatures were determined by plotting the first derivative of the absorbance versus the temperature curve.

The synthesized oligonucleotides for biochemical experiments are given in Figure 1, while Table 1 and Figure 1 show the sequences of the oligonucleotides that were used for hybridization studies. The Dickerson dodecamer (see Fig. 6) was used for NMR structural analysis.

Mass spectrometry and exact mass measurements

Quadrupole/orthogonal-acceleration time-of-flight tandem mass spectrometer (Q-Tof-2, Micromass, Manchester, UK), equipped with a standard electrospray-ionization (ESI) interface: the composition of the modified oligonucleotides was verified by ESI-MS analysis of samples infused in $^{I}PrOH/H_2O$ 1:1 at 3 µl min^{-1}.

Molecular modeling

The modified monomer with a thymine base was created using Macromodel 5.0 (7). The geometry was optimized in the Amber* force field (8). The atomic charges to be used in the Amber calculations were obtained from a Gamess run (9) followed by a RESP calculation (10). The parameter database used in Amber is the 1999 parameter set (11). The monomer was then fitted onto the residues 8 and 20 of a B-duplex ds(CGCGAATTCGCG) created by the Nucgen program. The energy of the resulting duplex was then minimized, while restraining the Watson–Crick hydrogen bonds and also by fixing the positions of the non-modified nucleotides. Eleven counter-ions (Na^+) were added and the duplex was inserted in a box of TIP3P waters (12) with initial dimensions 51 × 48 × 69 Å. The solvent around the duplex was then relaxed by a short energy minimization (1000 steps) using the Sander program. Then a molecular dynamics run of 500 ps at 300 K was started. All Sander MD calculations were performed with Sander_classic using periodic boundary conditions and using the particle mesh Ewald (PME) method for the summation of the coulomb interactions. The average structure was fitted on the NMR structure by superimposing the atoms, r.m.s. = 2.3 Å (Quatfit program in CCL software archives). To investigate the possibility of introducing a modified nucleotide in the template strand without obstructing the incorporation of new nucleotides in the primer strand, a modeling study was performed. At this moment, no ternary complex structures of the Klenow fragment of polymerase I of *Escherichia coli* have been published (13). Therefore we selected the ternary complex of DNA polymerase I from *Thermus aquaticus* (pdb code 3KTQ) (14). Template nucleotide GT4 was replaced by the nucleotide with the extra ribose sugar and the complementary incoming nucleotide triphosphate ddCTP was replaced by an adenine phosphate. Both nucleotides were modeled in the A conformation. A short energy minimization in Amber revealed a clash between the extra ribose and arg-746 which could not be resolved by simple energy minimization. Manually repositioning the arginine side chain by modifying the dihedral angles (χ_1 137, χ_2 –27.6) removed the conflict. A comparison of polymerase sequences (15) and a detailed examination of the structures of Klenow fragment of *E.coli* (1kfd) and *Taq* polymerase I (5ktq) reveals that arg-841 *E.coli* overlaps with arg-746 in *Taq* polymerase I, showing our model based on *Taq* polymerase to be a good representation of the active site in the *E.coli* polymerase I.

CD experiments

CD spectra were measured with a Jasco 600 spectropolarimeter in thermostatically controlled 1 cm cuvettes connected to a Lauda RCS6 bath. The oligomers were dissolved and analyzed in a solution of NaCl (0.1 M) and K_2HPO_4 (0.2 M, pH 7.5) at a concentration of 4 mM for each strand.

NMR analysis

Sample preparation. The modified self-complementary oligonucleotide strand was dissolved in D_2O and the pD was adjusted to 7.2. The sample was lyophilized and redissolved in 0.25 ml D_2O, resulting in a concentration of the strand of 3.4 mM. The solution was briefly heated to 80°C and slowly

Table 1. Thermal stability of dsDNA and DNA·RNA duplexes with modified (T*) and unmodified nucleotides

	r(5′-CCAGUGAUAUGC-3′)		d(5′-CCAGTGATATGC)-3′	
	T_m	ΔT_m mod^{-1}	T_m	ΔT_m mod^{-1}
d(5′-GCATATCACTGG-3′)	48.8°C	–	49.7°C	–
d(5′-GCATATCACT*GG-3′) (12)	45.0°C	–3.8°C	44.0°C	–5.7°C
d(5′-GCAT*AT*CACT*GG-3′) (13)	39.6°C	–3.1°C	33.4°C	–5.4°C
d(5′-GCATAT*CACTGG-3′) (14)	45.5°C	–3.3°C	44.4°C	–5.3°C

cooled to room temperature to promote duplex formation. For spectra in H_2O, the sample was again lyophilized and dissolved in 0.25 ml 90%H_2O/10%D_2O.

NMR spectroscopy. Spectra were recorded on a Varian 500 Unity spectrometer (operating at 499.140 MHz). Unless stated otherwise, spectra were recorded at 20°C. Quadrature detection was achieved in States-Haberkorn hypercomplex mode (16). Spectra were processed using the FELIX 97.00 software package (Biosym Technologies, San Diego, CA) running on a Silicon Graphics O2 R10000 workstation (IRIX version 6.3).

The 1D spectra in H_2O were recorded using a jump-return pulse as the observation pulse (17). The 2D NOESY in H_2O (mixing time = 200 ms; at 5°C) was recorded using the watergate watersuppression (18) with a sweep width of 10 000 Hz in both dimensions, 80 scans, 2048 data points in t_2 and 256 FIDs in t_1. The data were apodized with a shifted sine-bell square function in both dimensions and processed to a 2 K × 1 K matrix.

The 2D DQF-COSY (19), TOCSY (20) and NOESY (21) spectra in D_2O were recorded with a sweep width of 4200 Hz in both dimensions. The residual HDO peak was suppressed by low power, on resonance, presaturation during 800 ms. The DQF-COSY spectrum consisted of 2048 data points in t_2 and 1024 increments in t_1. The data were apodized with a shifted sine-bell square function in both dimensions and processed to a 2 K × 2 K matrix. Both ^{31}P-decoupled (on resonance, continuous decoupling) and ^{31}P-coupled spectra were recorded under the same conditions. For the TOCSY experiment, a clean MLEV17 (22) version was used, with a low power 90° pulse of 25.8 µs and the delay set to 72.8 µs. The total TOCSY mixing time was set to 65 ms. The spectrum was acquired with 32 scans, 2048 data points in t_2 and 256 FIDs in t_1. The data were apodized with a shifted sine-bell square function in both dimensions and processed to a 2 K × 1 K matrix. The NOESY experiments were acquired with mixing times of 50, 100, 150 and 250 ms, 32 scans, 2048 data points in t_2 and 400 increments in t_1.

A ^{1}H-^{31}P HETCOR (23) spectrum was acquired with 64 scans, 2048 data points in the proton dimension, t_2, and 256 increments in the phosphorus dimension, t_1, over sweep widths of 4200 and 1600 Hz, respectively. The data were apodized with a shifted sine-bell square function in both dimensions and processed to a 2 K × 1 K matrix.

NMR derived restraints. Distance restraints were derived from NOESY spectra recorded with 50, 100 and 150 ms mixing times, using the FELIX 97.00 based on the build-up curves, inter-proton distances were calculated. A relatively wide experimental error (±20%) was used on the calculated inter proton distances. The calibration of NOE cross peak intensities was done against the H5–H6 cross peaks as an internal standard and resulted in 320 intra-residue restraints and 96 inter-residue (six of which are inter-strand). Hydrogen bond restraints were used in stable base pairs and are implemented as NOE distance restraints.

Sugar puckers of the deoxyriboses in the DNA strand were inferred from the strong H1′ to H2′ (~9 Hz) and weak H3′ to H4′ (~2–3 Hz) scalar couplings and indicate S puckering of the sugar rings. The inserted ribose however shows coupling constants, characteristic for N type sugars [$J_{H1'\text{-}H2'}$ (~3.2 Hz), $J_{H2'\text{-}H3'}$ (~6.4 Hz), $J_{H3'\text{-}H4'}$ (~8.4 Hz)]. A pseurot analysis of this coupling data shows an equilibrium between N (70%) and S (30%) conformers (24,25). Dihedral restraints on H1′-C1′-C2′-H2" (157 ± 20°) and H2"-C2′-C3′-H3′ (–35 ± 20°), to define the S-type ribose conformation, and on H1*-C1*-C2*-H2* (99 ± 20°) and H2*-C2*-C3*-H3* (38 ± 20°), to define the N-type ribose conformation, were used for the structure determination.

The β torsion angles of the duplex were restrained (to 180 ± 30°) based on the observable four bond $J_{H4\text{-}P(n)}$ couplings (~4 Hz), indicating a W-shaped conformation of the atoms P-O5′-C5′-C4′. The small passive couplings observed in the H5′ to H5" cross peaks in the DQF-COSY spectrum and the nicely resolved H4′-P(n)-cross peak in the 2D ^{1}H-detected [^{1}H,^{31}P] correlation spectrum, allowed us to restrain the γ torsion angles in the DNA duplex to 60 ± 35°. The ε torsion angles were restrained (to 230 ± 70°) based on steric arguments. The ^{31}P chemical shifts were used to restrain α and ζ torsion angles (0 ± 120°). The torsion angles θ1, θ2, θ3, θ4, θ5 and θ6 were not restrained.

Since both strands of the duplex showed identical NMR properties, symmetry restraints were applied on the C1′ atoms of all deoxyribose moieties (26,27).

Structure determination. All structure calculations were performed with X-PLOR V3.851 (28). The topallhdg.dna and parallhdg.dna files were adapted to include the modified residue. In the topology file, a new residue, consisting of a thymidine with an extra ribose ring attached to its 3′ end, was introduced. This residue was subsequently patched into the oligonucleotide sequence in a way comparable to the treatment of RNA and DNA in the standard X-PLOR program. The modeled structure of the modified duplex was used to derive energy constants.

After the torsion angle molecular dynamics round (29), the majority of the structures (62%) had converged to very similar structures with similar total energies (274–384 kcal mol^{-1}) and no violations of the NOE and dihedral restraints. The 25 lowest energy structures were used for further refinement during the 'gentle molecular dynamics' round.

The final refinement started with a 20 ps constant temperature molecular dynamics simulation at 300 K (20 000 steps of 0.001 ps) and was followed by a 200-step conjugate gradient energy minimization of the average structure of the last 10 ps of the 20 ps simulation.

An analysis of the obtained 3D-structure with the computer programs X3DNA and CURVES 5.3, was used to compare the modified structure with the structure of the non-modified Dickerson dodecamer, that is extensively described in literature (30). Finally, some visual representations of the molecule were obtained with Molscript 1.4 and Bobscript 2.4.

Biochemical experiments

KFexo$^-$ DNA polymerase I reactions. Hybridization was performed combining the 5′-end labeled primer with their template in a molar ratio of 1:2.5. Strains were denatured by heating at 70°C for 10 min and annealed by slow cooling to room temperature during 2.5 h. Reactions were initiated by adding 3 µl of enzyme dilution to a reaction mixture of 6 µl consisting of hybrid, reaction buffer (supplied with the enzyme) and 6 µl of triphosphate building block. The highly

purified 2′-deoxyribonucleoside triphosphates used in the incorporation assay were from Pharmacia.

The incorporation experiments were set up to investigate whether the Klenow fragment of DNA polymerase I without 3′-5′ exonuclease activity (KFexo$^-$) (Promega) was able to incorporate a natural nucleotide building block into hybrid 1:2 (Fig. 1) opposite its unnatural complement in the template and to further extend with natural nucleotides. In these series of insertion assays, first dATP was added. The reaction mixture (10 µl) contained 50 nM hybrid 1:2, 10 µM dATP, reaction buffer and 0.5 U per µl KFexo$^-$. The sample was incubated at 37°C. After 30 min, 4 µl of dTTP (25 µM) or dCTP (25 µM) or dGTP (25 µM) or dCTP + dTTP (all 25 µM) or dGTP + dTTP or dCTP + dGTP (all 25 µM) or dCTP + dTTP + dGTP (all 25 µM) was added and the reaction was quenched after 1 h.

Digestion reactions. Hybridization of the 5′-end labeled primer with its template was performed as described above in a molar ratio of 1:1. Enzymatic reactions were started by addition of enzyme dilution to the reaction mixture. The final reaction volume contained 0.1 µg hybrid 3:4 or 3:5 or 2:4 or 2:5 and 1 or 10 U MboI or DpnII (all from New England Biolabs). The aliquots were incubated at 37°C. After 10, 30 and 120 min, the reaction was quenched.

Oxidation reaction—PAGE. 100 pmol [^{32}P]oligonucleotide 2 was dissolved in 100 µl $NaIO_4$ (500 mM) and incubated at 37°C for 3.5 h. The oligonucleotide was precipitated by adding 100 µL $LiClO_4$ (2 M) and 1 ml acetone. The mixture was stored at 4°C for 30 min. The sample was centrifuged for 5 min and the upper layer was removed. Subsequently, the sample was treated with base by addition of 18 µl of NaOH (0.1 M) (sample reaches pH 12). After 1 h at room temperature, the sample was adjusted to pH 7 by addition of 2 µl of KH_2PO_4 (1 M). The hybrid mixture was prepared by addition of 27.5 µl of H_2O and 2.5 µl of oligonucleotide 4 (10 µM). The mixture was heated for 10 min at 75°C followed by slow cooling to room temperature. The ligation reaction was performed at room temperature in 15 µl reaction volume containing 12 µl hybrid mixture, 1.5 µl 10× T4 DNA ligase reaction buffer (provided with the enzyme) and 1.5 µl T4 DNA ligase (400 U µl^{-1}, New England Biolabs). After 1 h, an aliquot was removed from the reaction mixture and mixed with a double amount of loading buffer. Then 1.5 µl of MboI restriction enzyme (10 U µl^{-1}, New England Biolabs) was added and the sample was kept at room temperature for 60 min. The reaction was quenched after 30 and 60 min by addition of a double amount of loading buffer. The samples were analyzed using PAGE and phosphor imaging.

Oxidation reaction—mass spectrometry. In two separate tubes, 10 nmol oligonucleotide 2 was dissolved in 200 µl $NaIO_4$ (500 mM) and incubated at 37°C for 3.5 h. The oligonucleotide following was precipitated by addition of 200 µl $LiClO_4$ (2 M) and 1 ml acetone. The mixture was stored for 30 min at 4°C. After centrifugation of the sample for 5 min, the upper layer was removed. One sample was dissolved in 5 µl of water, whereas the other sample was treated with base. Then 30 µl of NaOH (0.1 M) was added (sample reaches pH 12). After 1 h at room temperature, the sample was adjusted to pH 7 by addition of 4 µl of KH_2PO_4 (1 M). Both samples were desalted by means of a NAP-5™ column (Pharmacia) and further purified with RP-HPLC (Purospher® Star RP-18 endcapped, 3 µm, Merck) using a gradient of 0–0.015 TEAB in 30 min. The samples were then lyophilized.

Mass spectrometric analysis of oligonucleotides. Oligonucleotides were characterized and their purity was checked by HPLC/MS on a capillary chromatograph (CapLC, Waters, Milford, MA). 150 mm × 0.3 mm columns (LCPackings, San Francisco, CA) were used. Oligonucleotides were eluted with a triethylammonium-1,1,1,3,3,3-hexafluoro-2-propanol/acetonitrile solvent system. Flow rate was 5 µl min^{-1}. Electrospray spectra were acquired on an orthogonal acceleration/time-of-flight mass spectrometer (Q-Tof-2, Micromass, Manchester, UK) in negative ion mode. Scan time used was 2 s. The combined spectra from a chromatographic peak were deconvoluted using the MaxEnt algorithm of the software (Masslynx 3.4, Micromass, Manchester, UK). Theoretical oligonucleotide masses were calculated using the monoisotopic element masses.

Electrophoresis. During enzymatic incorporation assays, samples were removed and reactions were terminated by adding a double volume of loading buffer (95% formamide, 0.05% Bromophenol Blue, 0.5 xylene cyanol, and 50 mM EDTA). The products were heat denatured at 70°C for 5 min and separated on a 0.4 mm 20% denaturing polyacrylamide gel, in the presence of a 100 mM Tris–borate and 2.5 M EDTA buffer, pH 8.3, at 2000 V for ~2 h. Visualization of the polymerized products was done with a phosphor imager. The amount of radioactivity in the bands representing the respective polymerized products of enzymatic reactions was determined with Optiquant image analysis software (Packard, Perkin Elmer).

RESULTS

Oligonucleotide synthesis and hybridization studies

Preparation of the nucleoside phosphoramidites as well as incorporation into oligonucleotides was straightforward and according to standard procedures.

Hybridization studies revealed considerable destabilization of DNA duplexes upon incorporation of the modification (ΔT_m = 5.5°C mod^{-1}) and slightly less within a dsRNA context (ΔT_m= 3.5°C mod^{-1}) (Table 1). The sequence did not seem to have a lot of influence, as incorporation of the modification between two pyrimidines likewise resulted in a 5.7°C mod^{-1} drop in stability for the duplex 9:10 in comparison with the control duplex 8:10 (data not shown).

The modified Dickerson dodecamer, used in the NMR studies, shows a biphasic melting transition at sodium chloride concentrations of 0.01 M (T_{m1} < 30°C and T_{m2} = 65°C at 260 nm) and 0.1 M (T_{m1} = 30°C and T_{m2} = 69°C at 260 nm) whereas a biphasic transition of the unmodified control sequence could only be seen at 0.01 M (T_{m1} = 40°C and T_{m2} = 62°C at 260 nm). At higher salt concentrations both melting transitions overlap and only one transition is observed. The lower T_m corresponds to the transition from a duplex into two hairpins while the higher T_m results from denaturation of the hairpin into a single strand (31,32).

Table 2. Definition of the torsion angles in nucleotides depicted in Scheme 1

Backbone torsion angle	Involved atoms	Endocyclic torsion angle	Involved atoms
θ_1	C4′-C3′-O3′-C1*	ν_0	C4*-O4*-C1*-C2*
θ_2	C3′-O3′-C1*-C2*	ν_1	O4*-C1*-C2*-C3*
θ_3	C3*-C4*-C5*-O5*	ν_2	C1*-C2*-C3*-C4*
θ_4	C4*-C5*-O5*-P	ν_3	C2*-C3*-C4*-O4*
θ_5	C5*-O5*-P-O5′$_{(n+1)}$	ν_4	C3*-C4*-O4*-C1*
θ_6	O5*-P-O5′$_{(n+1)}$-C5′$_{(n+1)}$		

Atoms (n+1) belong to the adjacent C9(21) residue.

Our results show the first transition of the modified strand to occur at a lower temperature than the first melting transition of the control sequence, indicating a destabilization of the duplex structure due to the insertion of the extra ribose moiety. This corresponds to the destabilization seen in duplexes that are not able to form hairpin structures (Table 1). For the second melting transition, the modified sequence displays a higher T_m than the control. Thus, introduction of the studied modification increases the stability of the hairpin structure. These results are in agreement with the increase in thermal stability of hairpin structures by the introduction of a propanediol linker (abasic site) in the backbone of the loop (33).

Higher concentrations of the modified strand, as present in the NMR sample (3.4 mM), tend to increase T_{m1}. At 20°C, a stable duplex structure could be observed by NMR spectroscopy as spectra show stable base pair formation and regular base stacking in the central AT rich region of the modified Dickerson sequence.

Structural characterization using CD spectrometry

Circular dichroism may give initial information on the helix types that are involved during hybridization of nucleic acids. Before starting the NMR experiment, CD spectra were taken from the Dickerson dodecamer with and without incorporation of a disaccharide nucleoside at position 8 (20). Both spectra are very similar with a positive Cotton effect around 220 and 290 nm and a negative Cotton effect around 250 nm (see Supplementary Material). The intensity of the bands is decreased by increasing temperature and the natural double-stranded DNA is showing somewhat higher temperature stability, in agreement with its higher T_m. The similarity of both spectra suggests that there are no major differences in the geometries between both duplexes and that NMR analysis should mainly focus on the differences around the insertion site of the disaccharide nucleotide.

Structure determination by NMR spectroscopy

A high resolution structure of a modified Dickerson dodecamer with the self-complementary sequence: 5′d(CGCGAATT*CGCG)-3′ was determined using NMR spectroscopy (see Fig. 6). The modification is represented by T* and consists of an extra sugar ring, that is inserted at the regular phosphodiester linkage between T8(T20) and C9(C21). The atom numbering, chemical structure and main torsion angles of the modified part of the duplex are defined in Scheme 1 and Table 2. The selected sequence, 5′d(CGCGAATT*CGCG)-3′, is identical to the sequence used in the molecular modeling

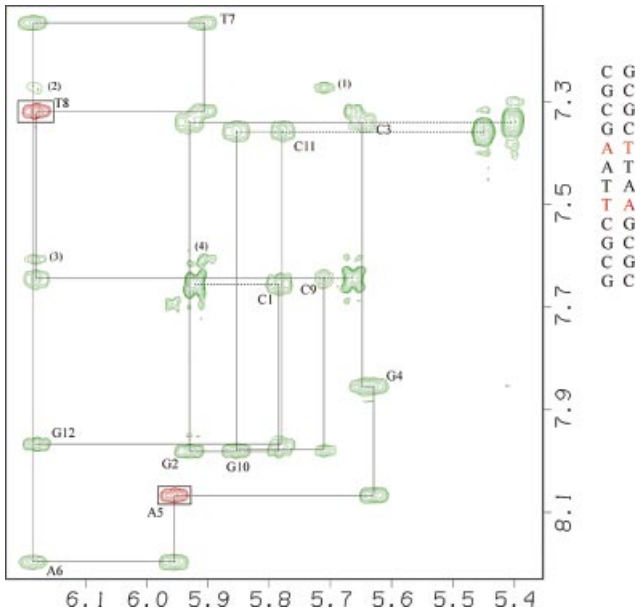

Figure 2. Portion of the 2D NOESY spectrum obtained in D_2O (250 ms mixing time, 20°C) showing the aromatic to H1′ cross peak region. The sequential walk along the H1′ and aromatic H6/H8 protons in the DNA strand is traced out by the continuous line. Peaks with a significant frequency shift compared to the non-modified helix are boxed. Assignments of cytosine H5 are indicated by broken lines. Assignment of marked cross peaks: H2:A6(18)-H1′:C21(9) (1), H2:A6(18)-H1′:T*20(8) (2), H2:A5(18)-H1′:T*20(8) (3) and H2:A5(18)-H1′:T19(7) (4).

studies and contains all four different nucleobases, occurring in DNA.

Non-exchangeable protons in the modified Dickerson dodecamer could be assigned starting from a standard anomeric to aromatic proton walk (26,27). Sequential connectivities for the entire DNA strand could be achieved (Fig. 2) and provided assignments for H1′, H5, H6 and H8 protons. The other protons of the spin systems were assigned from TOCSY, DQF-COSY and NOESY spectra (34). The ^{31}P resonances were assigned from the 2D ^{1}H-detected [^{1}H,^{31}P] correlation spectrum (HETCOR). Strong coupling could be observed between P and H3′ of the previous residue and between P and H4′ of the next residue (see Supplementary Material). The C9(21) phosphorus is strongly downfield shifted. Comparison of the resonance frequencies from the modified duplex to those of the corresponding signals from the non-modified dodecamer in similar experimental conditions, reveals that altered proton and phosphorus shifts are situated at

Table 3. Structure determination statistics for each set of 25 structures after refinement with all experimental restraints and hydrogen bonding between base pairs

	All restraints
Total energy (kcal mol^{-1})	61.9 ± 4.8
NOE violations (>0.5 Å)	0
Dihedral violations (>5°)	0 ± 0
RMSD from distance restraints (Å)	0.027 ± 0.001
RMSD from dihedral restraints (°)	0.198 ± 0.052
RMSD from average structure for all heavy atoms (Å)	0.566 ± 0.093

the modification site [residues T*8(20) and A5(17)]. These local changes in resonance frequencies can be related to local structural changes at the site of modification, while the rest of the duplex is hardly influenced by the extra ribose in the sugar-phosphate backbone.

In the deoxyriboses, strong COSY peaks were observed from H1′ to H2′, H2′ to H2" and from H5′ to H5" whereas the inserted ribose showed strong COSY peaks from H3′ to H4′ and from H5′ to H5". One-dimensional imino-proton spectra recorded at various temperatures in 90% H_2O/10% D_2O showed five sharp signals and one broad signal between 12.5 and 14 p.p.m. (see Supplementary Material). The five sharp signals could be assigned via imino-H1′ and imino-to-Adenine H2 cross peaks in the 2D watergate-NOESY, which was confirmed by an imino-to-imino sequential proton walk (results not shown). The remaining signal belongs to G12(24):H1. Fraying at the helix ends causes the broadening of this signal. The thermal stability of imino protons is characteristic for stable base pairing in the central part of the duplex that includes the modified site. Typical NOE interactions of the base protons with a continuous aromatic to anomeric and aromatic to aromatic proton walk is observed and is indicative of regular base-stacking in a B-type helical structure. To calculate the structure of 5′-d(CGCGAAT-T*CGCG)-3′ we performed torsion angle molecular dynamics (29) followed by a refinement of 25 selected structures using the NMR-derived restraints in X-PLOR 3.851, as described in Materials and Methods. During the structure calculation, experimental restraints were implemented to retrain inter-proton distances and sugar conformations. In the modified region, NOE contacts could be observed between H1*:T*8(20) and H3′:T*8(20), H1*:T*8(20) and H4′:T*8(20), H1*:T*8(20) and H5":T*8(20), H3*:T*8(20) and H4′:C9(21) and between H3*:T*8(20) and H5":C9(21). During calculation, the structures converged to a family of structures with similar geometry. Structure determination statistics are listed in Table 3.

Incorporation of dATP opposite unnatural complement and further extension with natural nucleosides

In a series of insertion experiments, it was investigated whether the natural adenosine nucleotide could be inserted opposite its unnatural complement. Likewise, further elongation with natural nucleotides was examined (Fig. 3). In a first step, dATP was added to the reaction mixture containing a final concentration of 50 nM hybrid 1:2, reaction buffer, 10 µM dATP and 0.5 U per µl KFexo$^-$. Lane 2 represents the incorporation profile using dATP in the reaction mixture at a

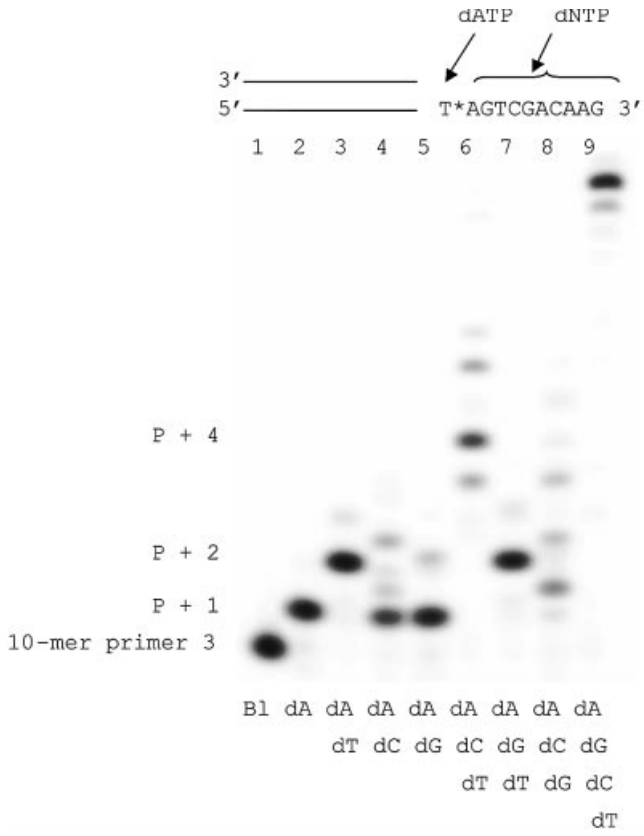

Figure 3. Phosphor image representing the insertion of dATP opposite its unnatural complement (T*) and further extension with natural nucleotides. The reaction mixture contained 50 nM hybrid 1:2, triphosphate building block, reaction buffer and 0.5 U per µl KFexo$^-$. The sample was incubated at 37°C. Lane 1 represents the blank reaction, lane 2: dATP (final concentration 10 µM) was added to the reaction mixture and the reaction time was 30 min. Lanes 3–9 show insertion profiles in the presence of dATP + dTTP (lane 3), dATP + dCTP (lane 4), dATP + dGTP (lane 5), dATP + dCTP + dTTP (lane 6), dATP + dGTP + dTTP (lane 7), dATP + dCTP + cGTP (lane 8) and dATP + dGTP + dCTP + dTTP (lane 9).

reaction time of 30 min. It can be observed that the original 10mer primer is completely elongated with one building block indicating that a natural adenosine nucleotide indeed can be inserted efficiently opposite its unnatural complement. To evaluate further extension with natural nucleotides following incorporation, dTTP (lane 3), dCTP (lane 4) or dGTP (lane 5) or a mixture of two (lanes 6–8) or three (lane 9) triphosphate building blocks were subsequently added to the reaction mixture. The results demonstrate that further elongation with natural dNTPs is indeed successful.

Digestion reactions

To evaluate whether the modified oligonucleotides 2 and 5 can be recognized by restriction enzymes, hybrids 2:5 or 3:5 or 2:4 were exposed to MboI and DpnII, both having a recognition site present in the hybrid (5′-GATC-3′) in which thymidine is replaced with the unnatural analogue in chains 2 and 5. At several time points, aliquots were removed from the reaction mixture and the reaction was quenched. The resulting products were separated by means of PAGE and visualized by phosphor imaging (Fig. 4). The images obtained indicated the MboI was

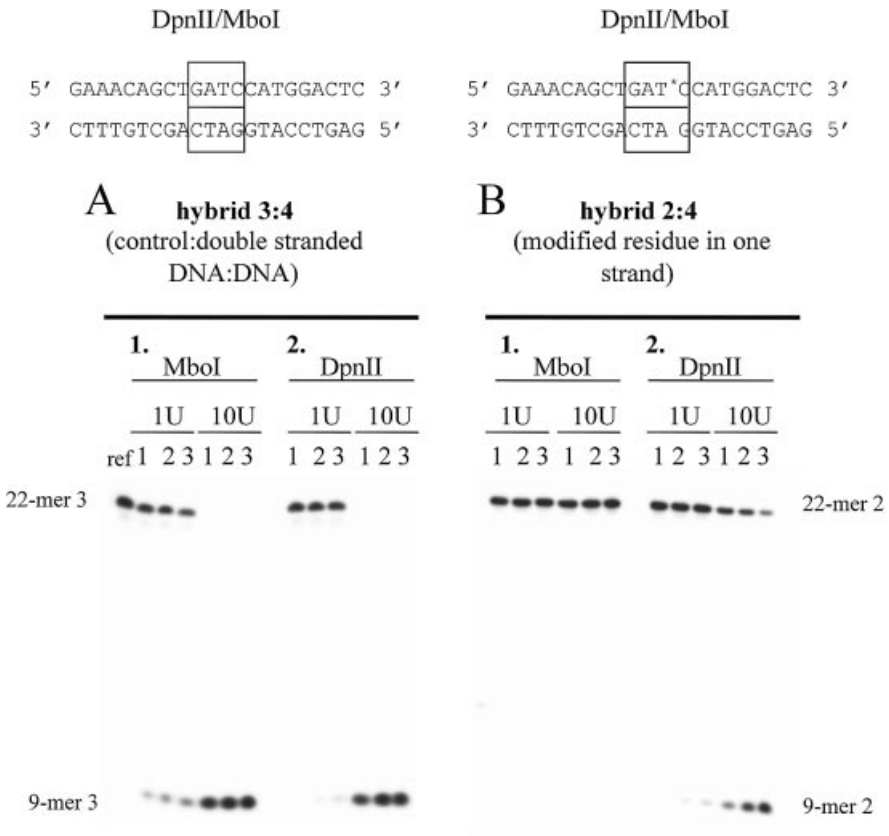

Figure 4. Digestion pattern in the presence of 0.1 µg hybrid 3:4 (**A**) or 2:4 (**B**) and 1 or 10 U MboI or DpnII (indicated on top of phosphor image). The reaction temperature was 37°C and the reaction time 10 (lane 1), 30 (lane 2) or 120 min (lane 3).

not active on either of the considered hybrids, except for the control double-stranded DNA/DNA (3:4) (Fig. 4A1). In contrast, DpnII was not only able to digest the natural double-stranded DNA/DNA (3:4) (Fig. 4A2), but also cleaved hybrids 2:4 (Fig. 4B2) and 3:5 (data not shown) although with a lower efficiency in comparison to the natural substrate. However, it did not succeed in digesting hybrid 2:5 containing the modified residue in both strands (data not shown).

Oxidation reactions

Two tests were designed to examine the susceptibility of oligonucleotide 2 to specific cleavage by oxidation at the site containing the modified nucleotide followed by a removal of the sugar residue in a hydrolysis using base treatment that would lead to formation of two (natural) oligomers 6 and 7 having, respectively a free 3′ hydroxyl group and a free 5′ phosphate group. In a first test, this reaction was evaluated using PAGE and phosphor imaging. When oligonucleotide 2 indeed is cleaved and the sugar residue removed, a shorter radioactively labeled 12mer chain (6) is obtained that can be separated using PAGE and visualized using phosphor imaging. To investigate whether the obtained cleavage products had the desired 3′-hydroxyl group (6) and 5′-phosphate group (7), a ligation reaction, using the 22mer oligonucleotides 4 as complement, was performed in the presence of T4 DNA ligase. T4 DNA ligase can only link two chains in which the donor chain is provided with a free 3′-hydroxyl group and the acceptor chain carries a 5′-phosphate group. Since these ends are only generated when cleavage of oligonucleotide 2 and concomitant removal of the sugar residue is achieved, ligation indicates the success of this reaction. First, oligonucleotide 2 was oxidized following a previously published procedure (35). In contrast to the method described in the literature, 100 µl $NaIO_4$ (500 mM) was used for the oxidation of 100 pmol of oligonucleotide 2 at a reaction time of 3.5 h. Following oxidation, the oligonucleotide was precipitated using $LiClO_4$ and acetone. After storage of 30 min at 4°C, the sample was centrifuged for 5 min and the upper layer was removed. The obtained sample was treated with NaOH (0.1 M) allowing cleavage of the oxidized product and resulting in a removal of the extra sugar residue. This cleavage was detected by separation of compounds in the sample by PAGE and visualization with phosphor imaging. A spot could be observed at a position referring to the natural 12mer DNA 6, but other cleavage products could also be seen (Fig. 5, lane 2). The yield of this cleavage reaction is almost quantitative since only 3% of the original 22mer was not cleaved during reaction. Figure 5, lane 3 shows the separation profile after ligation of the products obtained after oxidation and base treatment. A spot is generated at a higher position referring to the natural oligonucleotide 2. The cleavage products, generated by oxidation and subsequent base treatment that could be ligated, represent 29%. Lanes 4, 5 and 6 give digestion patterns in the presence of MboI after 30 min (lane 4), 1 h (lane 5) and 2 h (lane 6). The results show that the upper spot has disappeared and a lower spot (referring to the natural 9mer

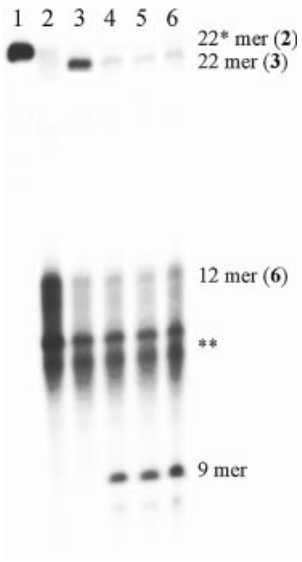

Figure 5. Phosphor image evaluating the oxidation reaction followed by ligation of the oxidized products and digestion with MboI. Lane 1 represents oligonucleotide 2; lane 2 shows the sample after oxidation of oligonucleotide 2. Lane 3 gives the separation pattern after ligation reaction. Lanes 4, 5 and 6 give profiles after digestion in the presence of MboI for 30 min (lane 4), 1 h (lane 5) and 2 h (lane 6). **Oligonucleotides obtained after oxidation and subsequent base treatment that could not be ligated using the 22mer oligonucleotide 4 as a complement.

oligonucleotide) is generated. Since it was previously shown that MboI was only able to digest the natural oligonucleotide 3 and could not cleave construct 2 (Fig. 4), this result further confirms the formation of the natural oligonucleotide 3 following ligation.

The formation of two natural oligonucleotides having, respectively, a free 3′-hydroxyl group (6) and a free 5′-phosphate group (7) upon oxidation and base treatment of construct 2, was further proven using mass spectrometry. After oxidation and base treatment for 1 h, the sample was desalted and further purified using RP-HPLC. The chromatogram showed two major peaks that were separately analyzed by mass spectrometry. One peak was identified as the desired 10mer oligonucleotide having a phosphate group at the 5′ position (7), whereas the other peak referred to the desired 12mer with a free hydroxyl group at its 3′ position (6). The sample that was dissolved in water following the oxidation reaction was also analyzed using mass spectrometry. The ESI-MS and deconvoluted spectrum revealed the presence of the uncleaved oxidized oligonucleotide 2 (see Supplementary Material).

DISCUSSION

Cleavage of DNA using chemical reagents is base-specific and not sequence-specific and results in the degradation of the nucleotide at the cleavage site. The most important examples of such cleavage reagents are used in sequencing methods. Other examples are anti-tumoral agents degrading DNA of fast growing cells (i.e. bleomycin). These cleavage reactions result in loss of genetic information because the reagents are chemically modifying the nucleotides. Cleavage of RNA at specific sites can be done using ribozymes. The selectivity of the cleavage site is determined by the selection of the sequence of the oligonucleotide. However, due to the absence of the 2′-OH group, this approach is difficult to use for DNA. The chemical cleavage of a phosphodiester bond within DNA at a specific position and without loss of nucleobase information, can be achieved using sugar-modified nucleotides. Such a method might be useful for the introduction of single-stranded nicks in double-stranded DNA (i.e. for the insertion of modified oligonucleotide fragments) or for the introduction of double-stranded nicks in double-stranded DNA (i.e. for restriction site cleavage). An important related question is the characterization of the duplex geometry at the modified site, which can be studied by NMR spectrometry.

The synthesis of the protected modified nucleoside (3′-O-β-D-ribofuranosyl-2′-deoxythymidine) was described previously (5). The 5′-position is protected with a monomethoxytrityl group and the 2*-OH and 3*-OH groups are protected with a benzoyl group. The 5*-OH group was converted into its phosphoramidite. This reagent was used for the synthesis of the oligonucleotides 2, 5 and 9 from Figure 1 and the modified oligonucleotides from Table 1. Oligonucleotide 11 (Fig. 6) represents the Dickerson sequence and was used for structural analysis. Mass spectrometry shows the correct incorporation of the modified nucleotide for all oligodeoxynucleotides (see Supplementary Material).

From Table 1, it is clear that incorporation of a disaccharide in an oligonucleotide leads to a decrease in duplex stability of ~3.4°C (with RNA as complement) and ~5.5°C (with DNA as complement). Therefore, we started structural studies in order to evaluate in which way the supplementary ribose unit influences local geometry of the duplex. In particular, the base pairing system should be retained for the fidelity of the polymerase reaction. CD analysis demonstrates that there is no fundamental difference in geometry between natural DNA duplex and the duplex with an inserted disaccharide nucleotide. Molecular dynamics using the Dickerson dodecamer, shows the formation of a stable duplex, from which the extra ribose sugar adopts a 2′-endo conformation. This unexpected result motivates a more profound study using NMR spectroscopy using the same Dickerson dodecamer.

Using all experimental NMR restraints, a structure calculation was performed. The structure closest to the average structure of 25 refined structures is shown in Figure 6. Obviously, insertion of an extra ribose in the phosphodiester linkage between T*8(20) and C9(21) causes only minor changes in the sugar phosphate backbone except from the modified site itself. The overall final structure remains a B-type helix. As in the original DNA Dickerson dodecamer, all deoxyribose rings occur in their C2′-endo puckering mode. The inserted ribose shows C3′-endo puckering. The extra ribose increases the length of the T8(20)–C9(21) linkage with several bonds. An overlay of the regular phosphodiester linkage between T8(20) and C9(21) in the non-modified Dickerson dodecamer and the modified linkage between T*8(20) and C9(21), demonstrates that the ‘new’ linkage is able to mimic the connection of two nucleosides by a natural phosphodiester bridge (Fig. 7). The extra ribose ring is folded out of the sugar phosphate backbone. It allows to close the gap between T*8(20) O3′ and C9(21) O5′ without major changes in the positions of T*8(20) and C9(21) deoxyribose

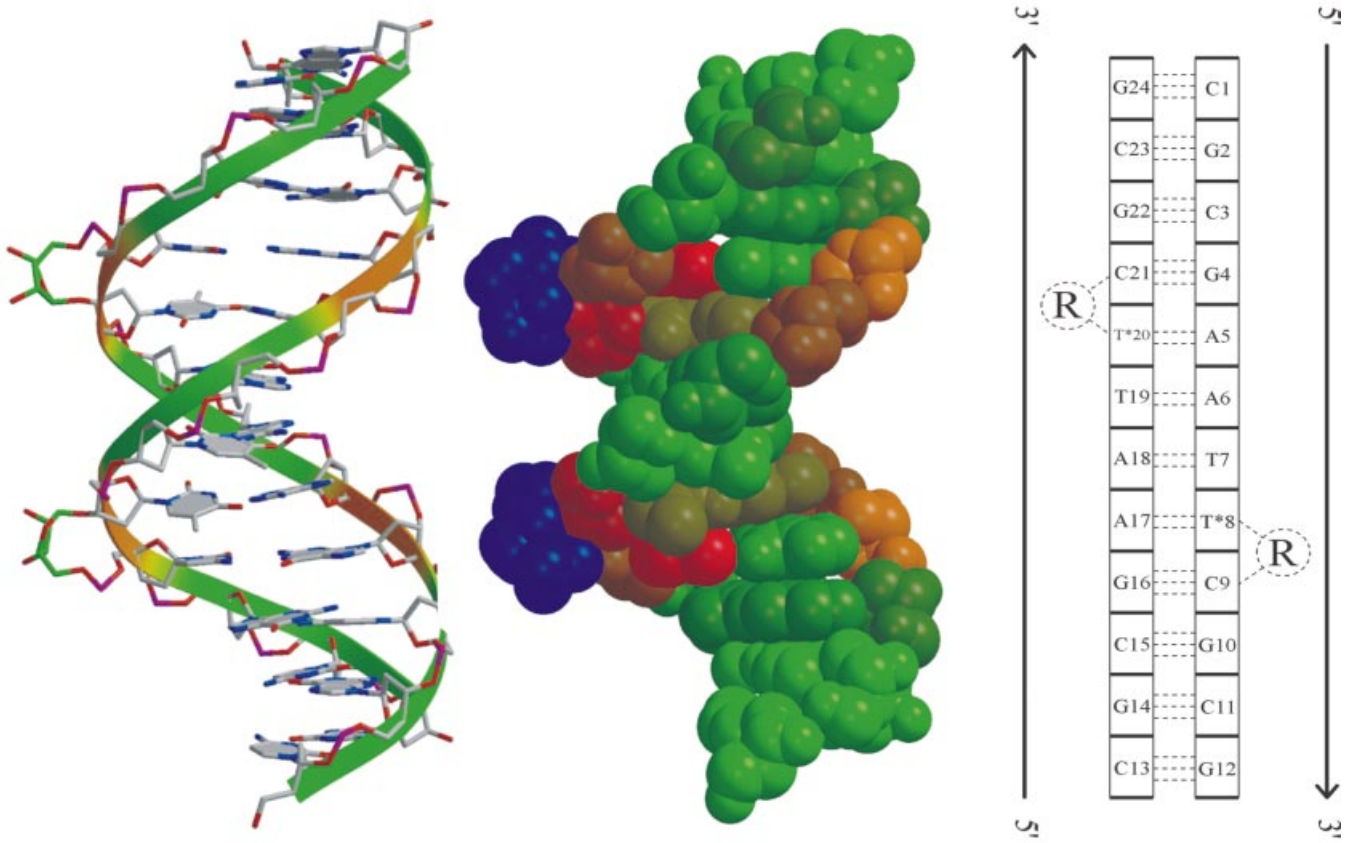

Figure 6. A visual representation of the 3D structure obtained by NMR spectroscopy. Left structure: a ribbon was drawn through the C4′ atoms of each deoxyribose moiety. The inserted ribose is colored green. The ribbon shows a green color in the portion of the structure where only minor differences in helical parameters exist between the modified and non-modified Dickerson dodecamer. A red color of the ribbon indicates a larger difference in helical parameters. Right structure: spacefill representation of the structure. Bases and sugars are colored as a function of their chemical shifts. A large difference in chemical shift between modified and unmodified molecules is indicated in red. Small differences are indicated by a green color. The inserted ribose is blue. Phosphates are not drawn.

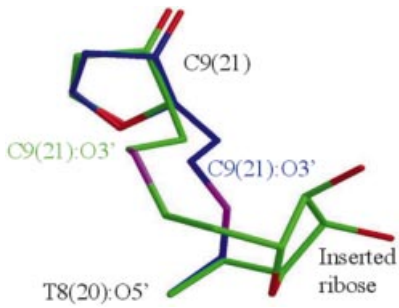

Figure 7. An overlay of the regular phosphodiester linkage between T8(20) and C9(21) in the non-modified Dickerson dodecamer (blue) and the modified linkage between T*8(20) and C9(21) (green). Sugar oxygens are colored in red and phosphorus atoms in magenta.

nucleosides in the duplex structure. This explains the normal base pairing and stacking behavior observed in the NMR spectra and the localized chemical shift changes.

Comparison of the helical parameters of the determined NMR structure with that of the non-modified Dickerson dodecamer, which is described in the literature, shows a good resemblance. A comparison of the propeller angle and helical shift of both structures shows that significant differences can only be observed in the direct neighborhood of the modification (Fig. 6). A comparison of the structure obtained by NMR spectroscopy and the modeled structure shows an overall similarity between the structures. This was demonstrated in an overlay of the two structures (see Supplementary Material) (RMSD = 2.635 Å) and by comparison of the torsion angles and puckering modes of the duplex and the modified portion (see Supplementary Material). However, as mentioned before, the most striking difference between modeling and NMR results, is the puckering of the second ribose in the disaccharide residues 8 and 20. The deoxyriboses in both NMR and modeling structures, adopt the south conformation, as expected for monomers present in a B-helix. In the model, the extra ribose has an average puckering amplitude of 183° and a phase angle of 38°, corresponding to a 2′-endo conformation, while the NMR measurements result in an amplitude of 36° and a phase angle of 46°, which represents a 3′-endo conformation.

To investigate this discrepancy, we started a molecular dynamics simulation from the average NMR derived structure using the same parameters and conditions as in the model above. After less than 100 ps, the extra ribose unit has flipped from the North to the South conformation, where it stays (for

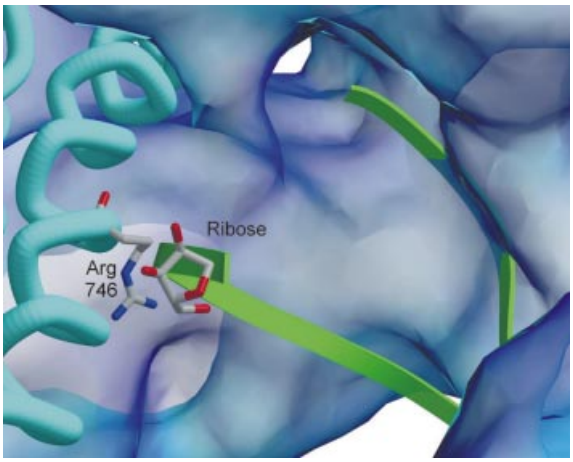

Figure 8. View inside the active site of the DNA polymerase I of *T.aquaticus*. The clash between the extra ribose and arg-746 could be resolved by repositioning the arginine side chain.

at least 400 ps of continued simulation). This ribose apparently prefers the 2′-endo conformation in the model and questions may be asked if this force field represents accurately this disaccharide structure. From both structural studies, it is clear, however, that the extra ribose is available in the duplex for cleavage reactions and that the base pairing system is retained.

In the biochemical experiments, we investigated the use of the modified oligonucleotide 2, hybridized with 1, for the incorporation of a natural nucleotide building block opposite the unnatural complement. Further elongation of this oligonucleotide was also studied. Opposite the disaccharide T* and using KFexo$^-$ DNA polymerase 1, a deoxyadenosine nucleotide was easily incorporated. Using a mixture of two nucleoside triphosphates (dATP and dTTP; dATP and dCTP; dATP and dGTP), we could show that further chain elongation with conservation of Watson–Crick base pair recognition is possible (lanes 3, 4 and 5 of Fig. 3). As must be clear from lanes 6 and 9 (Fig. 3), the whole DNA sequence could be filled in without major problems. Modeling experiments were performed to explain why a polymerase can successfully incorporate an adenosine residue opposite the modified T residue. The model reveals a clash between the extra ribose and arg-746 which could be resolved by repositioning the arginine side chain. Figure 8 shows a view inside the active site of the DNA polymerase I of *T.aquaticus*.

Two restriction enzymes were evaluated (MboI and DpnII) for their ability to cleave double-stranded DNA at the site where the disaccharide nucleotide is incorporated (sequence GATC). While MboI and DpnII were very efficient in cleaving the natural dsDNA, the incorporation of the disaccharide nucleotides (sequence GAT*C) slowed down the action of DpnII and abolished the enzymatic function of MboI. In the latter case, no cleavage could be detected. This enzyme was therefore used to control the ligation reaction after the cleavage at the extra ribose unit. Periodate is the preferred reagent for cleavage of vicinal diol functions. When oligonucleotide 2 was treated with periodate, a dialdehyde compound is obtained (Scheme 1). This compound could be detected using mass spectrometry. The dialdehyde oligo is further treated with 0.1 M NaOH (pH 12) resulting in the removal of the extra ribose unit and formation of two oligonucleotides, one with a 3′-OH function and the other with a 5′-*O*-phosphate group. The labeled oligo with the 3′-OH group is a 12mer that can be detected by gel electrophoresis. Both oligos were also identified using mass spectrometry. It should be stressed however, that periodate cleavage of ribose nucleosides gives a mixture of ring-opening and ring-closing products (36). Further treatment with NaOH may increase the complexity of the mixture in a reaction that has not been studied at the level of nucleotides and oligonucleotides. It is clear that some of these products cannot be used for the ligation reaction, using the 22mer oligonucleotide 4 as complement.

Both oligonucleotides could be ligated with T4 DNA ligase using oligonucleotide 4 as the template. As can be seen in Figure 5, an oligonucleotide (lane 3) is obtained with reconstitution of the original chain length. In a final experiment, we proved that this oligonucleotide is intact. Indeed, hybridization with the oligonucleotide 4 and cleavage with restriction enzyme MboI, allows us to obtain the expected 9mer fragment. The MboI would not cleave when the disaccharide fragment was still present.

We can conclude that a regular DNA duplex can be obtained by insertion of an extra ribose residue between the 3′-OH of one nucleotide and the 5′-*O*-phosphate of the next nucleotide. The 5′ → 5* linked phosphodiester function renders this oligonucleotide stable against restriction enzyme cleavage at the insertion site. This oligonucleotide can be chemically cleaved at the extra ribose unit with the generation of a 3′-OH function and a 5′-*O*-phosphate group (the whole supplementary ribose unit is removed) so that an intact natural oligonucleotide is obtained after the ligation reaction. An NMR structure only shows minor changes of helix parameters at the insertion site because the ribose linkage is able to mimic very well the backbone connection between successive nucleotides of natural DNA. This disaccharide modification opens the possibility to chemically cleave DNA without loss of genetic information and to renew the DNA in its original state. It might therefore be used as a chemical restriction-site cleaver, to insert oligonucleotide fragments into DNA, as a sugar-alternative for interference footprinting or as an anchor for reporting groups after assembly of the oligonucleotide.

SUPPLEMENTARY MATERIAL

Supplementary Material is available at NAR Online.

ACKNOWLEDGEMENTS

The authors thank C. Biernaux for editorial help. Financial support from K.U. Leuven is gratefully acknowledged. K.N. is a research assistant of the FWO and E.L. is a postdoctoral fellow of the FWO. K.V. and V.K. are recipients of an IWT fellowship.

REFERENCES

1. Hayashibara,K.C. and Verdine,G.L. (1991) Template-directed interference footprinting of protein guanine contacts in DNA. *J. Am. Chem. Soc.*, **113**, 5104–5106.
2. Mascareñas,J.L., Hayashibara,K.C. and Verdine,G.L. (1993) Template-directed interference footprinting of protein thymine contacts. *J. Am. Chem. Soc.*, **115**, 373–374.

3. Min,C., Cushing,T.D. and Verdine,G.L. (1996) Template-directed interference footprinting of protein-adenine contacts. *J. Am. Chem. Soc.*, **118**, 6116–6120.
4. Storek,M.J., Suciu,A. and Verdine,G.L. (2002) 5-amino-2′-deoxyuridine, a novel thymidine analogue for high-resolution footprinting of protein–DNA complexes. *Org. Lett.*, **4**, 3867–3869.
5. Efimtseva,E.V., Shelkunova,A.A., Mikhailov,S.N., Nauwelaerts,K., Rozenski,J., Lescrinier,E. and Herdewijn,P. (2003) Synthesis and properties of phosphorylated 3′-O-beta-D-ribofuranosyl-2′-deoxythymidine. *Nucl. Nucl.*, **22**, 359–371.
6. Maurinsh,Y., Rosemeyer,H., Esnouf,R., Medvedovici,A., Wang,J., Ceulemans,G., Lescrinier,E., Hendrix,C., Busson,R., Sandra,P., Seela,F., Van Aerschot,A. and Herdewijn,P. (1999) Synthesis and pairing properties of oligonucleotides containing 3-hydroxy-4-hydroxymethyl-1-cyclohexanyl nucleosides. *Chem. Eur. J.*, **5**, 2139–2150.
7. Mohamadi,F., Richards,N.G.J., Guida,W.C., Liskamp,R., Lipton,M., Caufield,C., Chang,G. and Hendrickson,T. (1990) Macromodel—an integrated software system for modeling organic and bioorganic molecules using molecular mechanics. *J. Comput. Chem.*, **11**, 440–467.
8. Weiner,P., Kollman,P.A., Nguyen,D.T. and Case,D.A. (1986) An all atom force-field for simulations of proteins and nucleic-acids. *J. Comput. Chem.*, **7**, 230–252.
9. Schmidt,M.W., Baldridge,K.K., Boatz,J.A., Elbert,S.T., Gordon,M.S., Jensen,J.H., Koseki,S., Matsunaga,N., Nguyen,K.A., Su,S., Windus,T.L., Dupuis,M. and Montgomery,J.A.,Jr (1993) General atomic and molecular electronic-structure system. *J. Comput. Chem.*, **14**, 1347–1363.
10. Cieplak,P., Cornell,W.D., Bayly,C.I. and Kollman,P.A. (1995) Application of the multimolecule and multiconformational resp methodology to biopolymers—charge derivation for DNA, RNA and proteins. *J. Comput. Chem.*, **16**, 1357–1377.
11. Wang,J., Cieplak,P. and Kollman,P.A. (2000) How well does a restrained electrostatic potential (RESP) model perform in calculating conformational energies of organic and biological molecules? *J. Comput. Chem.*, **21**, 1049–1074.
12. Jorgensen,W.L., Chandrasekhar,J., Madura,J. and Klein,M.L. (1983) Comparison of simple potential functions for simulating liquid water. *J. Chem. Phys.*, **79**, 926–935.
13. Dzantiev,L. and Romano,L.J. (2000) A conformational change in E-coli DNA polymerase I (Klenow fragment) is induced in the presence of a dNTP complementary to the template base in the active site. *Biochemistry*, **39**, 356–361.
14. Li,Y.,Korolev,S. and Waksman,G. (1998) Crystal structures of open and closed forms of binary and ternary complexes of the large fragment of *Thermus aquaticus* DNA polymerase I: structural basis for nucleotide incorporation. *EMBO J.*, **17**, 7514.
15. Delarue,M., Poch,O., Tordo,N., Moras,D. and Argos,P. (1990) An attempt to unify the structure of polymerases. *Protein Eng.*, **3**, 461–467.
16. States,D.J., Haberkorn,R.A. and Ruben,D.J. (1982) A two-dimensional Nuclear Overhauser experiment with pure absorption phase in 4 quadrants. *J. Magn. Reson.*, **48**, 286–292.
17. Plateau,P. and Guéron,M. (1982) Exchangeable proton NMR without base-line distortion, using new strong-pulse sequences. *J. Am. Chem. Soc.*, **104**, 7310–7311.
18. Piotto,M., Saudek,V. and Sklenar,V. (1992) Gradient-tailored excitation for single-quantum NMR-spectroscopy of aqueous-solutions. *J. Biomol. NMR*, **2**, 661–665.
19. Rance,M., Sørensen,O.W., Bodenhausen,G., Wagner,G., Ernst,R.R. and Wütrich,K. (1983) Improved spectral resolution in COSY H-1-NMR spectra of proteins via double quantum filtering. *Biochem. Biophys. Res. Commun.*, **117**, 479–485.
20. Bax,A. and Davis,G. (1985) MLEV-17-based two-dimensional homonuclear magnetization transfer spectroscopy. *J. Magn. Reson.*, **65**, 355–366.
21. Jeener,J., Meier,B.H., Bachman,P. and Ernst,R.R. (1979) Investigation of exchange processes by 2-dimensional NMR-spectroscopy. *J. Chem. Phys.*, **71**, 4546–4553.
22. Griesinger,C., Otting,G. and Wütrich,K. (1988) Clean TOCSY for H-1 spin system-identification in macromolecules. *J. Am. Chem. Soc.*, **110**, 7870–7872.
23. Sklenar,V., Miyashiro,H., Zon,G., Miles,H.T. and Bax,A. (1986) Assignment of the P-31 and H-1 resonances in oligonucleotides by two-dimensional NMR-spectroscopy. *FEBS Lett.*, **208**, 94–98.
24. deLeeuw,F.A.A.M. and Altona,C. (1983) Computer-assisted pseudorotation analysis of 5-membered rings by means of proton spin spin coupling-constants—PROGRAM PSEUROT. *J. Comput. Chem.*, **4**, 428.
25. Haasnoot,C.A.G., de Leeuw,F.A.A.M., de Leeuw,H.P.M. and Altona,C. (1981) The relationship between proton-proton NMR coupling-constants and substituent electronegativities. 2. Conformational-analysis of the sugar ring in nucleosides and nucleotides in solution using a generalized karplus equation. *Org. Magn. Reson.*, **15**, 43.
26. Evans,J.N.S. (1995) *Biomolecular NMR Spectroscopy*. Oxford University Press, Oxford, UK, pp. 343–394.
27. Wijmenga,S.S., Mooren,M.W. and Hilbers,C.W. (1993) NMR of nucleic acids, from spectrum to structure. In Roberts,G. (ed.), *NMR of Macromolecules: A Practical Approach*. Oxford University Press, Oxford, pp. 217–288.
28. Brünger,A.T. (1992) *X-PLOR Version 3.1, A System for X-ray Crystallography and NMR*. Yale University Press, New Haven, CT.
29. Stein,E.G., Rice,L.M. and Brünger,A.T. (1997) Torsion-angle molecular dynamics as a new efficient tool for NMR structure calculation. *J. Magn. Reson.*, **124**, 154–164.
30. Tjandra,N., Tate,S.-I., Ono,A., Kainosho,M. and Bax,A. (2000) The NMR structure of a DNA dodecamer in an aqueous dilute liquid crystalline phase. *J. Am. Chem. Soc.*, **122**, 6190–6196.
31. Seela,F. and Kehne,A. (1987) Palindromic octa-nucleotides and dodecanucleotides containing 2′-deoxytubercidin—synthesis, hairpin formation and recognition by the endodeoxyribonuclease ecori. *Biochemistry*, **26**, 2232–2238.
32. Marky,L.A., Blumenfield,K.S., Kozlowski,S. and Breslauer,K.J. (1983) Salt-dependent conformational transitions in the self-complementary deoxydodecanucleotide d(CGCAATTCGCG)—evidence for hairpin formation. *Biopolymers*, **22**, 1247–1257.
33. Seela,F. and Kaiser,K. (1987) Oligodeoxyribonucleotides containing 1,3-propanediol as nucleoside substitute. *Nucleic Acids Res.*, **15**, 3113–3129.
34. Varani,G. and Tinoco,I. (1991) RNA structure and NMR-spectroscopy *Q. Rev. Biophys.*, **24**, 479–532.
35. Brevnov,M.G., Gritsenko,O.M., Mikhailov,S.N., Efimtseva,E.V., Ermolinsky,B.S., Van Aerschot,A., Herdewijn,P., Repyk,A.V. and Gromova,E.S. (1997) DNA duplexes with reactive dialdehyde groups as novel reagents for cross-linking to restriction-modification enzymes *Nucleic Acids Res.*, **25**, 3302–3309.
36. Ermolinsky,B.S. and Mikhailov,S.N. (2000) Periodate oxidation in chemistry of nucleic acids: dialdehyde derivatives of nucleosides, nucleotides and oligonucleotides (review). *Bioorg. Khim.*, **26**, 483–504.